Research Article | Vol. 27, No. 3 | 4 Feb 2019 | OPTICS EXPRESS 3247
Optics EXPRESS

Improvement of the intensity noise and frequency stabilization of Nd:YAP laser with an ultra-low expansion Fabry-Perot cavity

JUAN YU,[1] YUE QIN,[1] ZHIHUI YAN,[1,2] HUADONG LU,[1,2] AND XIAOJUN JIA[1,2,*]

[1] *State Key Laboratory of Quantum Optics and Quantum Optics Devices, Institute of Opto-Electronics, Shanxi University, Taiyuan, 030006, China*
[2] *Collaborative Innovation Center of Extreme Optics, Shanxi University, Taiyuan 030006, China*
[*] *jiaxj@sxu.edu.cn*

Abstract: Continuous-wave, single-frequency, solid-state lasers with long-term frequency stability and low-intensity noise are an essential resource to generate squeezed and entangled states of light. In order to obtain the stable, nonclassical states of light, the frequency of the laser has to be stabilized with a stable reference. Due to the zero expansion property at a certain temperature, an ultra-low expansion (ULE) Fabry-Perot (F-P) cavity with a high finesse can be used as one of the best candidates of the frequency reference. We perform a detailed analysis of an extraordinarily high-frequency stability and ultra-low-intensity noise laser based on an improved cascade Pound-Drever-Hall frequency stabilization to a ULE F-P cavity. The frequency drift of the laser is suppressed to 7.72 MHz in 4 hours, and the noise level of the laser is simultaneously reduced to the quantum noise limit in the frequency below 300 kHz, which provides the possibility for the direct generation of a stable, high-level squeezed state in a lower-frequency region.

1. Introduction

Nonclassical states of light including Einstein-Podolsky-Rosen (EPR) entangled state of light [1] and squeezed state of light [2–4] are essential resources for many applications, such as quantum information processing [5–9], quantum memory [10–12], quantum metrology and precise measurements [13–15]. Optical parametric down-conversion processing in an optical cavity is one of the most efficient methods for the generation of nonclassical states of light. Both squeezed state and EPR entangled state of light can be directly obtained from degenerate optical parametric amplifier (DOPA) or nondegenerate optical parametric amplifier (NOPA) [1,3,15–19]. Especially for the nonclassical states at wavelength of 1080 nm, they can be obtained with single NOPA because the light at this wavelength can realize type-II non-critical phase matching in a $KTiOPO_4$ (KTP) crystal without walk-off effect [1,16]. But in certain situations, for example, in gravitational wave detection [20–22] and interaction with the atomic media area [23,24], squeezed state in audio frequency band and below is required [25–27]. In the generation of the quadrature squeezed state in audio frequency band, McKenzie *et* al. [25] compared the parametric down-conversion with different seed powers and confirmed that the seed field leads to the degradation of the squeezing in low frequencies due to the high background noise which mainly derived from the relaxation oscillation of usual solid-state laser [17,18]. Thus, a low-noise and frequency-stablized solid laser is essential to offer the necessary pump field and seed field for DOPA and NOPA. Therefore, an effective way must be found to reduce the noise of the solid laser for improving the squeezing level in audio frequency band and below. In order to reduce the frequency drift and the extra noise of solid laser, an excellent frequency reference has to be selected. A high finesse Fabry-Perot (F-P) cavity, which has a wider and more flexible application due to its unlimited laser wavelength compared with atomic or molecular transition

#351254 https://doi.org/10.1364/OE.27.003247
Journal © 2019 Received 8 Nov 2018; revised 19 Dec 2018; accepted 2 Jan 2019; published 30 Jan 2019

Optics EXPRESS

spectral lines [28], is usually used as the reference cavity of the laser for transferring the frequency stability of the laser to the length stability of the cavity [29, 30].

We experimentally achieve the solid-state laser in an extraordinarily high stabitity and low noise by locking the laser to a spherical high finesse ultra-low expansion (ULE) F-P cavity with an special-designed cascade Pound-Drever-Hall (PDH) [31, 32] technique. An acousto-optic modulator (AOM) is used as the fast feedback actuator [33–35] to improve the response bandwidth of the locking system and a piezo-electric transducer (PZT) attached on a cavity mirror of the laser is used as the slow feedback actuator to improve the long-term stability of the system. The long-term frequency drift of the laser is suppressed to 7.72 MHz in 4 hours, and the noise level of the laser is simultaneously reduced to the quantum noise limit (QNL) from 1.5 MHz to 300 kHz which provides the possibility for stable high-level squeezed state in near-audio frequency region.

2. Experimental setup

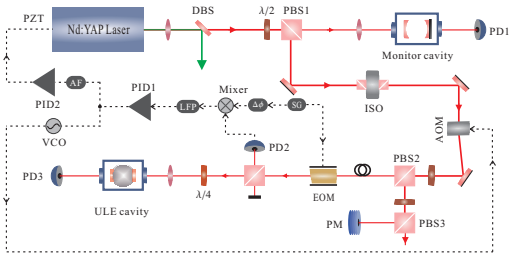

Fig. 1. Schematic of the experimental setup. Dotted curves and solid curves represent the circuitry part and the light path, respectively. Nd:YAP Laser: Intra-cavity frequency-doubled tunable single-frequency laser. DBS: Dichroic beam spliter. $\lambda/2$: Half-wave plate. $\lambda/4$: Quarter-wave plate. PBS1-3: Polarization beam splitter. EOM: Electro-optic modulator. ISO: Isolator. PZT: Piezo-electric transducer. PD1-3: Power detector. PM: Power meter. AOM: Acousto-optic modulator. PID1-2: Proportional-integral-differential controller. LPF: Low-pass filter. AF: Attenuation filter. VCO: Voltage controlled oscillator. SG: Signal generator. $\Delta\phi$: Phase shift. ULE cavity: Ultralow expansion cavity.

A schematic of our experimental setup is illustrated in Fig. 1. The laser source is a continuous wave intra-cavity frequency-doubled tunable single-frequency Nd:YAP/LBO solid-state laser with the wavelength outputs of both 1080 nm and 540 nm, which is provided by YuGuang company (CDPSSFG-VIB). The two output beams are separated by a dichroic beam spliter (DBS) coated with the films of high reflection (HR) at 540 nm and antireflection (AR) at 1080 nm. The 1080 nm laser is divided into two parts by a beam splitter consiting of a half-wave plate ($\lambda/2$) and a polarization beam splitter (PBS). One part of 1080 nm laser is injected into a monitor cavity with free spectral range (FSR) of 750 MHz for monitoring the single-frequency performance and measuring frequency drift of the laser. The remaining part firstly passes an optical isolator (ISO) and a AOM. The driving signal of AOM at 165 MHz is provided by a voltage controlled oscillator (VCO, Mini-Circuits, ZX95-200A-S+) and amplified with a high-power amplifier (Mini-Circuits, ZHL-1-2W+). The frequency-shifted first-order output light of the AOM is divided into two parts, one part is injected into a power meter (PM) to measure the long-term power stability of the laser and the other part is coupled to a single-mode polarization maintaining fiber. The output laser from the fiber is phase-modulated by an homemade electro-optic modulator (EOM) with resonating frequency of 16.4 MHz. Almost all EOMs generate some unwanted residual amplitude modulation (RAM) which results in the systematic zero base line drift (ZBD) of the PDH error signal [36]. An EOM with a wedged MgO: $LiNbO_3$ is designed to reduce the ZBD of the PDH error signal [37]. Due to the natural birefringence of the crystal, the ordinary beam

Optics EXPRESS

and the extraordinary beam can be seperated in space after the wedged face. Finally, the light is spatially mode-matched to the high finesse ULE F-P cavity by a lens with a focal length of 500 mm. The cavity from AT Films is a sphere made of Corning ULE glass that has a low thermal expansion coefficient specified to below $1 \times 10^{-8} \frac{1}{K}$ between 26 °C and 36 °C. It is constructed with fused silica mirror substrates, which can improve the frequency stability by decreasing the thermal noise. The length of the optical cavity is 50 mm, and resulting in a theoretical data 3 GHz FSR and 60 kHz linewidth. The cavity design is insensitive to both vibrations and orientation as described in [38]. State-of-the-art laser frequency stabilization by high finesse optical cavities is limited fundamentally by thermal noise induced cavity length fluctuations [39]. The ultrastable optical F-P cavity which acted as the optical frequency reference of laser is easily affected by the external environment disturbance, and the stability of the final optical frequency is limited by the F-P cavity length L,

$$\frac{\Delta f}{f} = \frac{\Delta L}{L}, \tag{1}$$

where f is the resonant frequency of the ULE F-P cavity, Δf is frequency fluctuation and ΔL is variation of cavity length. Since the laser frequency follows the resonant frequency of the reference cavity, the stability of the reference cavity length becomes essential to achieve ultra-high frequency stability [40]. Several approaches are made to prevent changes of the cavity length caused by acoustic and seismic noise. The cavity is placed in a vacuum chamber, held at a pressure of about 10^{-8} mbar. Heat convection inside the cavity is suppressed due to the vacuum and then the temperature stability is improved. In addition, the accuracy of the chamber temperature stability is achieved at 5 mK/°C. Because acoustics can directly couple into the setup via air, a box with two additional layers of acoustic shielding and vibration isolation materials is built around the vacuum system. The whole setup is placed on a pneumatic vibration isolator optical table.

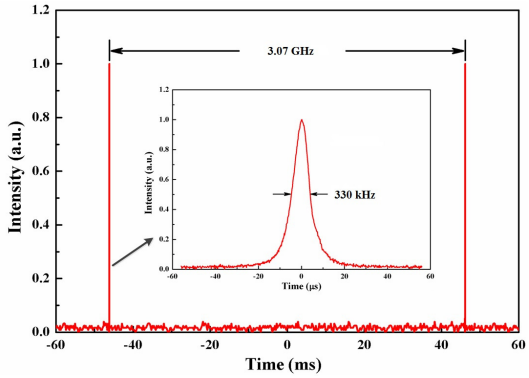

Fig. 2. The measured FSR of the ULE cavity and the linewidth of the laser .

At the same time, the high finesse F-P cavity provides a method to measure the linewidth of the solid laser when the linewidth of the laser is much wider than the linewidth of the ULE cavity. But the scan range of used laser is too short to scan a complete 3 GHz FSR of the ULE cavity. Therefore, we have improved the Nd:YAP/LBO laser by combining an intracavity etalon (IE) locked on a laser oscillating mode with intracavity nonlinear loss [41], and increasing an additional PZT (HPSt 150/14-10/55, Piezomechanik GmbH) with a longer elongation to expand the tuning range of the laser. The frequency tuning range is 6.3 GHz and 12.6 GHz for 1080 nm and 540 nm, respectively. That is to say, there are two PZTs attached on a cavity mirror of the laser, the long one for large-scale tuning and the short one used as the slow feedback actuator. In the experiment, the transmission peak of IE is firstly locked on the laser oscillating mode. And

Optics EXPRESS

then the output wavelength of laser can be tuned continuously by scaning the length of the long PZT to obtain a complete FSR of the ULE cavity. It can be seen that a complete FSR of the ULE cavity is 4.09 times of the 750 MHz FSR of the monitor cavity from the oscilloscope. The measured FSR of the ULE cavity is 3.07 GHz as shown in Fig. 2, which is in accordance with the theoretical calculation. Then the transmission mode of the ULE cavity is expended by adjusting the length of the two PZTs cooperatively. By comparing the full width half maximum (FWHM) of the transmission mode read from the oscilloscope with the 750 MHz FSR of the monitor cavity, the linewidth of the laser can be calculated to be 330 kHz as shown in the insert of Fig. 2.

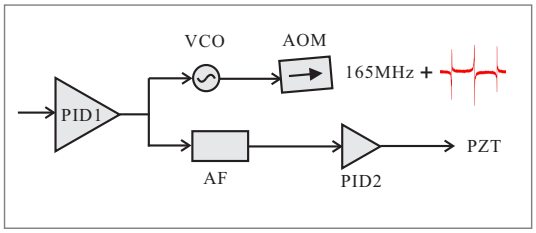

Fig. 3. Schematic of the partial servo controller. PID1-2: Proportional-integral-differential controller. AOM: Acousto-optic modulator. AF: Homemade attenuation filter. VCO: Voltage controlled oscillator. PZT: Piezo-electric transducer.

In our experiment, locking the laser to one of the ULE cavity modes is achieved by an improved cascade PDH technique. The short PZT of the laser and AOM are used as the slow and fast feedback actuators, respectively, which effectively improve the response bandwidth and optical frequency locking precision of the system. The phase-modulated 1080 nm beam via EOM is injected into the temperature-controlled ULE cavity, and the light reflected from the cavity is detected by PD2 which is obtained through the combination of a PBS and a quarter-wave plate ($\lambda/4$). The 16.4 MHz modulation signal output from the SG is divided into two parts, one part is used to drive the EOM and the other is first passed a phase shifter ($\Delta\phi$), and then mixed with the detected alternating-current (AC) signal to generate the error signal. The PDH error signal is derived by demodulating the AC signal detected by PD2 at 16.4 MHz. Here we use two types of the proportional-integral-differential controllers (PIDs), Vescent D2-125 (bandwidth > 10 MHz) and SIM 960 (bandwidth ~ 100 kHz), in the fast and slow servo loops, respectively. The critical problem is to make these two servo loops effeciently working and the detail of the servo controller is as shown in Fig. 3. The PDH error signal is performed by PID1 and divided into two parts, one part including the 165 MHz sinusoidal signal driven by the error signal is directly feedback to the VCO-controlled AOM for achieving the initial short-term locking of the laser. The other part of the error signal is injected into a homemade attenuation filter (AF) and the filtered low frequency part (below 2.5 kHz) is processed by a PID2 and then feedback to the PZT attached on a cavity mirror of the laser. The two loops are strictly chronological instead of simultaneously, which can improve the long-term stability of the locking system [42]. This method is used to compensate the variation of the cavity length and guarantee long-term frequency stability. At this point, we have completed the laser frequency stabilization with a high finesse F-P cavity by using the combination of PZT and AOM as the slow and fast feedback actuators, respectively, which effectively improve the response bandwidth of the locking system and the accuracy of optical frequency locking.

3. Results and discussion

In order to compare the effect of locking, the intensity noise power spectras of the 1080 nm laser (250 μW) are respectively measured with and without locking the laser to the ULE cavity. The detection system includs a 50/50 beam splitter (50/50 BS) and a pair of homemade high

Optics EXPRESS

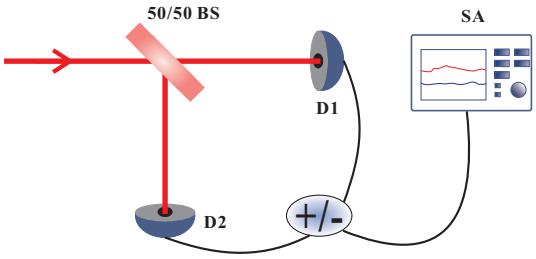

Fig. 4. Schematic of the intensity noise power spectra detection system. 50/50 BS: 50/50 beam splitter. D1-2: Homemade high signal-to-noise ratio detector. +/-: Positive or negative power combiner. SA: Spectrum analyzer.

signal-to-noise ratio (SNR) detectors (D1 and D2), as shown in Fig. 4. The optical field to be measured is first divided into two equal parts through 50/50 BS, and then injected into D1 and D2 separately. The outputs of the two detectors are added through the positive power combiner to obtain the intensity noise power spectra and the corresponding QNL is obtained by subtracting the two outputs through a negative power combiner [43, 44]. The intensity noise depicted by relative intensity noise (RIN) [45, 46] which the noise is scaled to the average power level of light is measured and recorded by a spectrum analyzer (SA) with resolution bandwidth (RBW) of 30 kHz and video bandwidth (VBW) of 30 Hz as shown in Fig. 5. The black, red and blue curves correspond to the QNL, the intensity noise power spectras of the laser with and without locking the laser to the ULE cavity, respectively. When the laser is freely running, we can see that the intensity noise is higher than the QNL when the analysis frequency is below 1.5 MHz. When the frequency of the laser is locked to the ULE F-P cavity, the noise level of the laser is reduced from 4.8 dB/Hz above the QNL to the QNL at 300 kHz (see the insert of Fig. 5), ensuring a RIN level reached the minimum -148 dB/Hz for frequencies above 300 kHz.

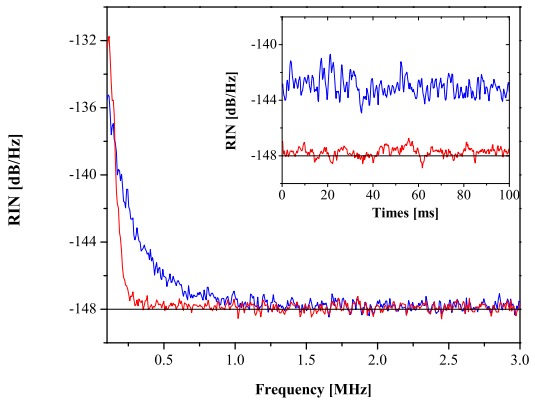

Fig. 5. The intensity noise power spectras of the laser state.

The frequency drift of the output laser is reduced to 9.84 MHz in 1 minute via feedback control to a nonlinear loss deliberately introduced to the laser resonator for the all-solid-state continuous-wave single-frequency lasers [47], which is too short for completing the measurement of noise spectra in low frequency. Thus, a long-term frequency stability is necessary. In the process of the experiment, the longitudinal-mode structure of the laser is always monitored by the monitor cavity, and the frequency stability of the laser is recorded, which is as shown in Fig. 6. The upper part shows the 750 MHz FSR of the monitor cavity (the horizontal scale is 5

Optics EXPRESS

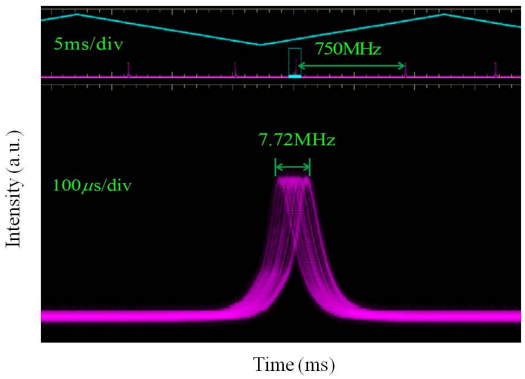

Fig. 6. Frequency drift of the 1080 nm laser in 4 hours.

ms), the lower part shows the frequency drift of the laser (the horizontal scale is 100 μs). By comparing the horizontal distance read from the oscilloscope of the upper and lower parts, the frequency drift can be calculated. The frequency drift is less than 7.72 MHz in 4 hours with the laser is locking to the high finesse ULE cavity, which proves an obviously improved frequency stability. The laser system can work continuously for more than 4 hours and the long term power stability of the laser is recorded by a PM and data acquisition system, as shown in Fig. 7. The root-mean-square (RMS) fluctuation over 4 hours is less than 0.41% and the measured power stability is less than ±0.92% in 4 hours in Fig. 7(a). Allan deviation [48] associated with the power stability at the averaging time from 0.125 s to 2000 s is as shown in Fig. 7(b). The power stability of the laser reached the minimum 1.35×10^{-3} for an integration time of 128 seconds.

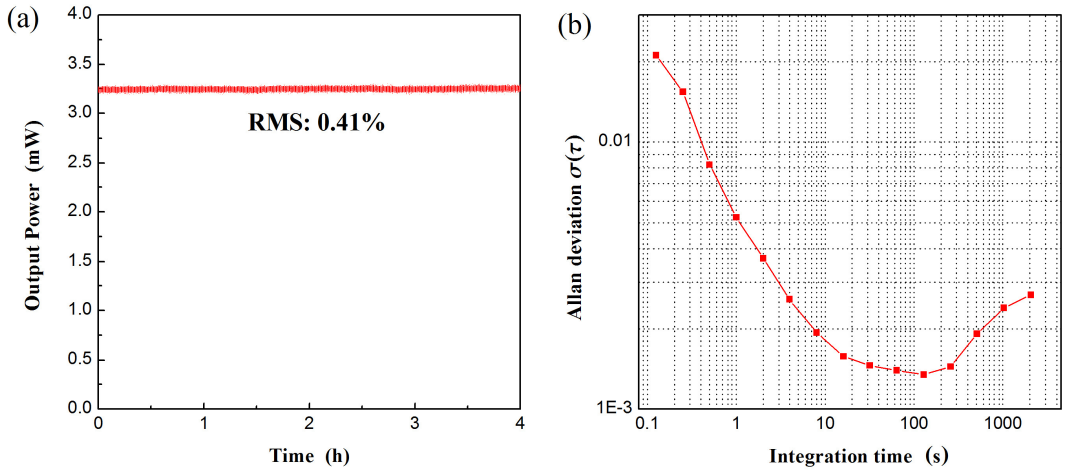

Fig. 7. Power stability of the laser in 4 hours.

4. Conclusion

With a cascade PDH laser stabilization system, the Nd:YAP laser operating at 1080 nm is frequency-stabilized to a high finesse ULE F-P cavity via fast feedback to an AOM and slow feedback to the PZT in the laser cavity and the laser system can continuously work for more than 4 hours. The noise level of the laser is reduced to the QNL at 300 kHz, and the frequency drift

Optics EXPRESS

is less than 7.72 MHz in 4 hours, which provides a stable optical source for the generation of high-level squeezed state in near-audio frequency. In the near future, we would like try to improve the squeezing level in near-audio frequency with this laser and develope a stable nonclassical light resource with this stable laser system.

Funding

National Key R&D Program of China (2016YFA0301402), the National Natural Science Foundation of China (11474190, 11654002, 61775127 and 11834010), the Program for Sanjin Scholars of Shanxi Province and the Fund for Shanxi "1331" Project Key Subjects Construction.

References

1. Z. Y. Ou, S. F. Pereira, and H. J. Kimble, "Realization of the Einstein-Podolsky-Rosen paradox for continuous variables in nondegenerate parametric amplification," Appl. Phys. B. **55**, 265-278 (1992).
2. R. E. Slusher, L. W. Hollberg, B. Yurke, J. C. Mertz, and J. F. Valley, "Observation of squeezed states generated by four-wave mixing in an optical cavity," Phys. Rev. Lett. **55**(22), 2409-2412 (1985).
3. L. A. Wu, H. J. Kimble, J. L. Hall, and H. F. Wu, "Generation of squeezed states by parametric down conversion," Phys. Rev. Lett. **57**(20), 2520-2523 (1986).
4. S. Machida, Y. Yamamoto, and Y. Itaya, "Observation of amplitude squeezing in a constant-current-driven semiconductor lasers," Phys. Rev. Lett. **58**(10), 1000-1003 (1987).
5. S. L. Braunstein and P. van Loock, "Quantum information with continuous variables," Rev. Mod. Phys. **77**(2), 513-577 (2005).
6. A. Furusawa, J. L. Sorensen, S. L. Braunstein, C. A. Fuchs, H. J. Kimble, and E. S. Polzik, "Unconditional quantum teleportation," Science **282**, 706-709 (1998).
7. C. W. Chou, D. B. Hume, M. J. Thorpe, D. J. Wineland, and T. Rosenband, "Quantum coherence between two atoms beyond $Q = 10^{15}$," Phys. Rev. Lett. **106**(16), 160801 (2011).
8. Y. Y. Zhou, J. Yu, Z. H. Yan, X. J. Jia, J. Zhang, C. D. Xie, and K. C. Peng, "Quantum secret sharing among four players using multipartite bound entanglement of an optical field," Phys. Rev. Lett. **121**(15), 150502 (2018).
9. M. R. Huo, J. L. Qin, J. L. Cheng, Z. H. Yan, Z. Z. Qin, X. L. Su, X. J. Jia, C. D. Xie, and K. C. Peng, "Deterministic quantum teleportation through fiber channels," Sci. Adv. **4**, eaas9401 (2018).
10. Z. H. Yan, L. Wu, X. J. Jia, Y. H. Liu, R. J. Deng, S. J. Li, H. Wang, C. D. Xie, and K. C. Peng, "Establishing and storing of deterministic quantum entanglement among three distant atomic ensembles," Nat. Commun. **8**, 718 (2017).
11. K. Honda, D. Akamatsu, M. Arikawa, Y. Yokoi, K. Akiba, S. Nagatsuka, T. Tanimura, A. Furusawa, and M. Kozuma, "Storage and retrieval of a squeezed vacuum," Phys. Rev. Lett. **100**(9), 093601 (2008).
12. J. Appel, E. Figueroa, D. Korystov, M. Lobino, and A. I. Lvovsky, "Quantum memory for squeezed light," Phys. Rev. Lett. **100**(9), 093602 (2008).
13. H. Grote, K. Danzmann, K. L. Dooley, R. Schnabel, J. Slutsky, and H. Vahlbruch, "First long-term application of squeezed states of light in a gravitational-wave observatory," Phys. Rev. Lett. **110**(18), 181101 (2013).
14. K. Goda, O. Miyakawa, E. E. Mikhailov, S. Saraf, R. Adhikari, K. McKenzie, R. Ward, S. Vass, A. J. Weinstein, and N. Mavalvala, "A quantum-enhanced prototype gravitational-wave detector," Nat. Phys. **4**, 472-476 (2008).
15. T. Eberle, S. Steinlechner, J. Bauchrowitz, V. Händchen, H. Vahlbruch, M. Mehmet, H. Müller-Ebhardt, and R. Schnabel, "Quantum enhancement of the zero-area sagnac interferometer topology for gravitational wave detection," Phys. Rev. Lett. **104**(25), 251102 (2010).
16. Y. Y. Zhou, X. J. Jia, F. Li, C. D. Xie, and K. C. Peng, "Experimental generation of 8.4 dB entangled state with an optical cavity involving a wedged type-II nonlinear crystal," Opt. Express **23**(4), 4952-4959 (2015).
17. X. Wen, Y. S. Han, J. Y. Liu, J. He, and J. M. Wang, "Polarization squeezing at the audio frequency band for the Rubidium D_1 line," Opt. Express **25**(17), 20737-20748(2017).
18. M. Mehmet, S. Ast, T. Eberle, S. Steinlechner, H. Vahlbruch, and R. Schnabel, "Squeezed light at 1550 nm with a quantum noise reduction of 12.3 dB," Opt. Express **19**(25), 25763-25772 (2011).
19. H. Vahlbruch, M. Mehmet, K. Danzmann, and R. Schnabel, "Detection of 15 dB squeezed states of light and their application for the absolute calibration of photoelectric quantum efficiency," Phys. Rev. Lett. **117**(11), 110801 (2016).
20. R. Schnabel, N. Mavalvala, D. E. McClelland, and P. K. Lam, "Quantum metrology for gravitational wave astronomy," Nat. Commun. **1**(8), 121 (2010).
21. The LIGO scientific collaboration, "Enhanced sensitivity of the LIGO gravitational wave detector by using squeezed states of light," Nat. Photonics **7**, 613–619 (2013).
22. The LIGO scientific collaboration and the virgo collaboration, "Observation of gravitational waves from a binary black hole merger," Phys. Rev. Lett. **116**(6), 061102 (2016).
23. F. Wolfgramm, A. Cerè, F. A. Beduini, A. Predojević, M. Koschorreck, and M. W. Mitchell, "Squeezed-light optical magnetometry," Phys. Rev. Lett. **105**(5), 053601 (2010).
24. N. Otterstrom, R. C. Pooser, and B. J. Lawrie, "Nonlinear optical magnetometry with accessible in situ optical squeezing," Opt. Lett. **39**(22), 6533-6536 (2014).

Optics EXPRESS

25. K. McKenzie, N. Grosse, W. P. Bowen, S. E. Whitcomb, M. B. Gray, D. E. McClelland, and P. K. Lam, "Squeezing in the audio gravitational-wave detection band," Phys. Rev. Lett. **93**(16), 161105 (2004).
26. H. Vahlbruch, S. Chelkowski, K. Danzmann, and R. Schnabel, "Quantum engineering of squeezed states for quantum communication and metrology," New J. Phys. **9**, 371 (2007).
27. W. H. Yang, X. L. Jin, X. D. Yu, Y. H. Zheng, and K. C. Peng, "Dependence of measured audio-band squeezing level on local oscillator intensity noise," Opt. Express **25**(20), 24262-24271 (2017).
28. T. Horrom, R. Singh, J. P. Dowling, and E. E. Mikhailov, "Quantum-enhanced magnetometer with low-frequency squeezing," Phys. Rev. A **86**(2), 023803 (2012).
29. L. S. Chen, J. L. Hall, J. Ye, T. Yang, E. J. Zang, and T. C. Li, "Vibration-induced elastic deformation of Fabry-Perot cavities," Phys. Rev. A **74**(5), 053801 (2006).
30. D. G. Matei, T. Legero, S. Häfner, C. Grebing, R. Weyrich, W. Zhang, L. Sonderhouse, J. M. Robinson, J. Ye, F. Riehle, and U. Sterr, "1.5 μm lasers with sub-10mHz linewidth," Phys. Rev. Lett. **118**(26), 263202 (2017).
31. R. W. P. Drever, J. L. Hall, F. V. Kowalski, J. Hough, G. M. Ford, A. J. Munley, and H. Ward, "Laser phase and frequency stabilization using an optical resonator," Appl. Phys. B. **31**, 97-105 (1983).
32. E. D. Black, "An introduction to Pound-Drever-Hall laser frequency stabilization," Am. J. Phys. **69**(1), 79-87 (2001).
33. J. Millo, D. V. Magalhães, C. Mandache, Y. L. Coq, E. M. L. English, P. G. Westergaard, J. Lodewyck, S. Bize, P. Lemonde, and G. Santarelli, "Ultrastable lasers based on vibration insensitive cavities," Phys. Rev. A. **79**(5), 053829 (2009).
34. P. Ehlers, I. Silander, J. Y. Wang, and O. Axner, "Fiber-laser-based noise-immune cavity-enhanced optical heterodyne molecular spectrometry instrumentation for Doppler-broadened detection in the 10^{-12} cm^{-1} $Hz^{-1/2}$ region," J. Opt. Soc. Am. B. **29**(6), 1305-1315 (2012).
35. C. W. Chou, D. B. Hume, J. C. J. Koelemeij, D. J. Wineland, and T. Rosenband, "Frequency comparison of two high-accuracy Al^+ optical clocks," Phys. Rev. Lett. **104**(7), 070802 (2010).
36. I. Silander, P. Ehlers, J. Y. Wang, and O. Axner, "Frequency modulation background signals from fiber-based electro optic modulators are caused by crosstalk," J. Opt. Soc. Am. B. **29**(5), 916-923 (2012).
37. Z. X. Li, W. G. Ma, W. H. Yang, Y. J. Wang, and Y. H. Zheng, "Reduction of zero base line drift of the Pound–Drever–Hall error signal with a wedged electro-optical crystal for squeezed state generation," Opt. Lett. **41**(14), 3331-3334 (2016).
38. D. R. Leibrandt, M. J. Thorpe, M. Notcutt, R. E. Drullinger, T. Rosenband, and J. C. Bergquist, "Spherical reference cavities for frequency stabilization of lasers in non-laboratory environments," Opt. Express **19**(4), 3471-3482 (2011).
39. T. Kessler, C. Hagemann, C. Grebing, T. Legero, U. Sterr, F. Riehle, M. J. Martin, L. Chen, and J. Ye, "A sub-40-mHz-linewidth laser based on a silicon single-crystal optical cavity," Nat. Photonics **6**, 687-692 (2012).
40. C. Salomon, D. Hils, and J. L. Hall, "Laser stabilization at the millihertz level," J. Opt. Soc. Am. B. **5**(8), 1576-1587 (1988).
41. P. X. Jin, H. D. Lu, Q. W. Yin, J. Su, and K. C. Peng, "Expanding continuous tuning range of a CW single-frequency laser by combining an intracavity etalon with a nonlinear loss," IEEE J. Sel. Top. Quantum Electron. **24**(5), 1600505 (2018).
42. N. M. Sampas, E. K. Gustafson, and R. L. Byer, "Long-term stability of two diode-laser-pumped nonplanar ring lasers independently stabilized to two Fabry-Perot interferometers," Opt. Lett. **18**(12), 947-949 (1993).
43. Y. Wang, H. Shen, X. L. Jin, X. L. Su, C. D. Xie, and K. C. Peng, "Experimental generation of 6 dB continuous variable entanglement from a nondegenerate optical parametric amplifier," Opt. Express **18**(6), 6149-6155 (2010).
44. D. Wang, Y. N. Shang, Z. H. Yan, W. Z. Wang, X. J. Jia, C. D. Xie, and K. C. Peng, "Experimental investigation about the influence of pump phase noise on phase-correlation of output optical fields from a non-degenerate parametric oscillator," Europhys Lett. **82**, 24003 (2008).
45. S. Taccheo, G. Sorbello, and P. Laporta, "Suppression of intensity noise in a diode-pumped Tm–Ho:YAG laser," Opt. Lett. **25**(22), 1642-1644 (2000).
46. K. Audo and M. Alouini, "Intensity noise cancellation in solid-state laser at 1.5 μm using SHG depletion as a buffer reservoir," Appl. Opt. **57**(7), 1524-1529 (2018).
47. P. X. Jin, H. D. Lu, J. Su, and K. C. Peng, "Scheme for improving laser stability via feedback control of intracavity nonlinear loss," Appl. Opt. **55**(13), 3478-3482 (2016).
48. D. W. Allan, "Statistics of atomic frequency standards," P. IEEE, **54**(2), 221-230 (1966).